lipidology

MDPI

Article

Identification of Lipid Droplet-Associated Genes in Breast Cancer Patients

Senol Dogan [1,2,*,†], Jenny Leopold [3,†], Daniel T. Hoffmann [1], Hans Kubitschke [1], Eliane Blauth [1], Carlotta Ficorella [1], Amelie Zschau [4], Jürgen Schiller [3] and Josef A. Käs [1]

[1] Peter Debye Institute, Faculty of Physics and Earth Science, Leipzig University, Linnéstr. 5, 04103 Leipzig, Germany; daniel-hoff@outlook.de (D.T.H.); hans.kubitschke@uni-leipzig.de (H.K.); eliane.blauth@physik.uni-leipzig.de (E.B.); carlotta.ficorella@physik.uni-leipzig.de (C.F.); jkaes@uni-leipzig.de (J.A.K.)
[2] Department of Gynecology, Medical Center, University of Leipzig, 04103 Leipzig, Germany
[3] Institute for Medical Physics and Biophysics, Faculty of Medicine, Leipzig University, Härtelstr. 16-18, 04107 Leipzig, Germany; jenny.leopold@medizin.uni-leipzig.de (J.L.); juergen.schiller@medizin.uni-leipzig.de (J.S.)
[4] Werner-Heisenberg-Gymnasium Leipzig, Renftstraße 3, 04159 Leipzig, Germany; amelie.zschau@gmx.de
* Correspondence: senol.dogan@uni-leipzig.de
† These authors contributed equally to this work.

Abstract: Lipid droplets (LDs) are known to be involved in the invasion and migration of breast cancer (BC) cells. This study aimed to identify LD-associated genes as prognostic markers in BC through comprehensive literature research and integration with lipid composition studies in BC cell lines. The GEPIA platform was used to analyze the differential expression of LD-associated genes in BC. The lipid composition of cell lines (MCF-10A, MDA-MB 436 and 231) was obtained by extraction and thin-layer chromatography coupled with mass spectrometry (MS). Additionally, cell lines were co-cultured with fatty tissue and analyzed by confocal fluorescence microscopy. A total of 143 genes were identified as LD-associated genes through literature research and were subsequently analyzed using GEPIA. Among these, three genes were found to be over-expressed and 45 under-expressed in BC. Notably, *FABP7* showed a statistically significant rank for all bioinformatics criteria as a prognostic factor. Experimental results showed only minor changes from MCF-10A to both MDA-MB cell lines for apolar lipids (triacylglycerols and cholesteryl esters) compared to phospholipids (PLs). Microscopic analyses showed that MDA-MB-231 had larger LDs compared to MCF-10A after 10 days of cultivation. Our bioinformatics analysis identified 26 genes that play important roles in metastatic transition in BC via LD-related mechanisms, though these findings could be only partially confirmed by experimental lipid compositional analyses, so far.

Keywords: lipid droplet-associated genes; prognostic factors of breast cancer; lipid metabolism; mass spectrometry

Citation: Dogan, S.; Leopold, J.; Hoffmann, D.T.; Kubitschke, H.; Blauth, E.; Ficorella, C.; Zschau, A.; Schiller, J.; Käs, J.A. Identification of Lipid Droplet-Associated Genes in Breast Cancer Patients. *Lipidology* **2024**, *1*, 52–74. https://doi.org/10.3390/lipidology1010005

Academic Editor: Nicola Ferri

Received: 26 March 2024
Revised: 17 June 2024
Accepted: 21 June 2024
Published: 11 July 2024

1. Background

Breast cancer is the most prevalent cancer globally and affects millions of individuals, primarily women [1]. According to the World Health Organization (WHO), between 2015 and 2020, 7.8 million women were diagnosed with breast cancer, 2.3 million alone in 2020 [2]. Moreover, breast cancer, combined with metastases, resulted in a mortality of 685,000 individuals in 2020 [2]. Particularly in low- and middle-income countries, most women were diagnosed with breast cancer in later stages, accompanied by high mortality (approx. 62% deaths) [3]. There are two different possibilities for detecting cancer at an early stage: (1) early diagnosis of symptomatic afflictions at the onset of the breast cancer disease or (2) screening of a defined group, e.g., women of a defined age, to find asymptomatic stages of the disease in "healthy" individuals [4]. Due to the screening methods and potential

oncologic therapies (such as surgery, radiation, chemotherapy, and hormone therapy), the survival rate of women suffering from breast cancer has increased. Nevertheless, scientists continue to study promising treatments and drugs with new combinations of existing cures. For more details and "up-to-date" knowledge, the National Cancer Institute (NCI) website (www.cancer.gov, accessed on 2 May 2024) is highly recommended and a short summary of the most important parameters is given at the end of this study. DNA alterations (chromosomal rearrangements, mutations, epigenetic changes like activation or suppression of specific genes) are early indicators of the growth of cancer [5]. Over the past years, genomics and epigenomics research enabled the identification of aberrant genes and their crosslinks to different cancer types by next-generation sequencing [6]. The progress in DNA sequencing allowed the analysis of the breast tumor genome and the cataloging of these genetic mutations [7]. Since genes encode proteins, proteomics studies are commonly used to extend genomics and to understand protein–protein and protein–metabolite interactions in more detail [8]. Proteomics allows the identification of novel biomarkers from cancer patients' body fluids (normally blood) using their protein and peptide profile [9]. Unfortunately, to the best of our knowledge, there are so far only very few (protein) biomarkers to identify (early-stage) breast cancer [10,11]. Although the use of cell-free DNA from the serum was suggested to provide early-stage breast cancer biomarkers [12], this has (in our opinion) a disadvantage: even if the required DNA exists, this does not necessarily lead to the synthesis of the corresponding proteins and other metabolites.

In the last two decades, mass spectrometry (MS)-based lipidomic studies (as a part of the increasing metabolomics field) were established and used for the (quantitative) lipid analysis in health and disease [13]. Lipids serve various crucial functions in cells: they act as packing materials for cellular contents (glycerophospholipids in all biomembranes), play essential roles in energy storage (glycerolipids and particularly triacylglycerols), and function as secondary messenger molecules, e.g., free fatty acids and products derived thereof [14]. With improvements in lipidomic technology, i.e., the development of powerful and affordable mass spectrometers, the importance of lipids and their correlation with the onset of breast cancer could be elucidated in many studies, as recently reviewed [15]. Altered lipid compositions and/or alterations of the fatty acyl compositions seem to be promising indicators regarding breast cancer diagnosis. For instance, Silva and colleagues demonstrated that there are characteristic changes between breast cancer and control samples in the ratio of lysophosphatidylcholine (LPC) 16:0 to phosphatidylcholine (PC) 16:0/18:2 [16]. This suggests an increased activity of the enzyme phospholipase A_2 (PLA_2), which converts PC into LPC. The role of phospholipases in tumor progression is, thus, well established [17]. In a more general way, aberrant lipid synthesis and reprogrammed lipid metabolism are both associated with the development and progression of breast cancer [18,19]. There are two potential reasons: on the one hand, releasing free fatty acids from lipids and their subsequent oxidation might be essential to supply physiological processes with energy. Furthermore, the phospholipid bilayers are fundamental structural components important for transporting molecules into (or outside of) the cell and mediating cellular proliferation processes [20]. Lipid droplets (LDs) are ubiquitous intracellular organelles (which are seen mainly in cancer cells), which store neutral lipids such as triacylglycerols and cholesterol esters [20]. Moreover, LDs are involved in signaling, inflammation, and energy metabolism as well as storage, and play a crucial role in cancer cell proliferation [21].

The storage of neutral lipids in LDs is vital for protecting cells from lipotoxicity, due to the excessive buildup of lipids in cell membranes. This is particularly important because free fatty acids, for instance, act as detergents, and thus destabilize the structures of membranes [22,23]. Some genetic information regarding the regulation of LDs can be obtained from the enzymes and proteins responsible for lipid metabolism and LD formation. The focus of this work was to identify the genes related to LDs and to examine their expression and their role in metastatic transition and reveal potential prognostic

factors. Additionally, different cancer-relevant cell cultures were screened for their lipid compositions and the most pronounced changes were monitored for lipid fingerprinting. Although the initial focus was on apolar lipids, only minor changes could be detected. However, significant changes occurring in the patterns of phospho- and sphingolipids were monitored.

2. Methods

Bioinformatics and genomics data analysis were performed to find the potential LD-related gene activities in breast cancer patients. Next, MCF-10A, MDA-MB-231, and MDA-MB-436 cells were analyzed according to their lipid compositions by thin-layer chromatography coupled with mass spectrometry (TLC-MS). Lastly, the physical presence and chemical structure of LDs were microscopically examined in MCF-10A, MDA-MB-231, and MDA-MB-436 cells, which were co-cultivated with human primary adipose tissue. The complete procedure is summarized in Figure 1.

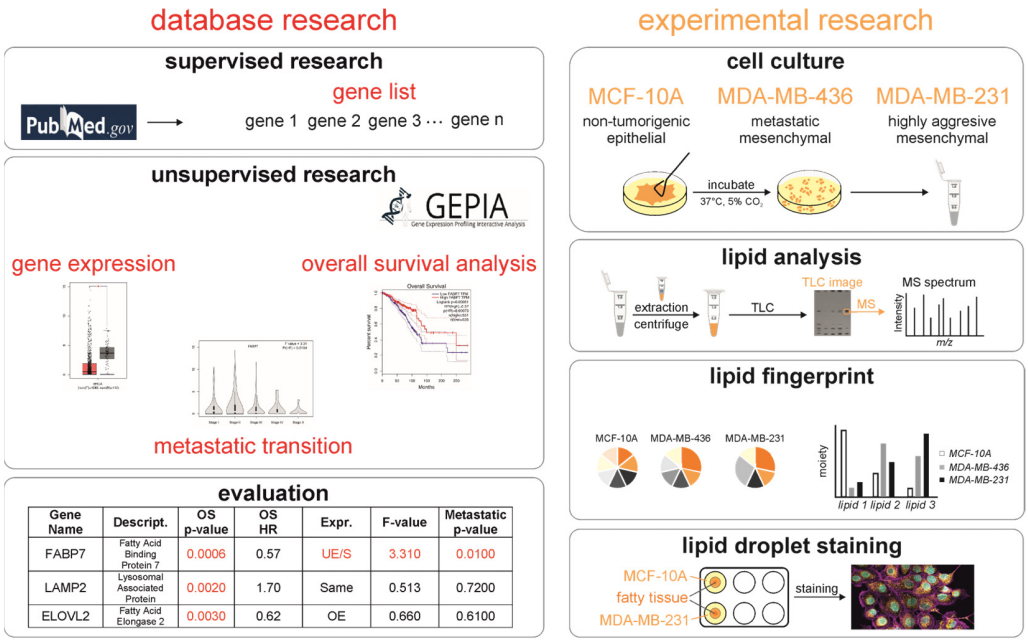

Gene Name	Descript.	OS p-value	OS HR	Expr.	F-value	Metastatic p-value
FABP7	Fatty Acid Binding Protein 7	0.0006	0.57	UE/S	3.310	0.0100
LAMP2	Lysosomal Associated Protein	0.0020	1.70	Same	0.513	0.7200
ELOVL2	Fatty Acid Elongase 2	0.0030	0.62	OE	0.660	0.6100

Figure 1. Overview of three different research aspects included in this study. The database search was first carried out by supervised searching using the PubMed platform to find all genes associated with breast cancer. Afterwards, different unsupervised research tools were used to define the characteristics of the genes found. The gene-expression-profiling interactive analysis (GEPIA, www.gepia.cancer-pku.cn) was used for gene expression levels and the overall survival (OS) analysis, and for differences in metastatic transitions and differential gene expression. The experimental part of this study included the cultivation of three different cell lines (MCF-10A, MDA-MB-436 and MDA-MB-231). The lipid extraction (according to the Folch extraction protocol [24] and analysis by TLC-ESI MS from the cell lines were used to create lipid fingerprints. At the end, similarities or differences between experimental and statistically gained results were identified and interpreted. In a third experiment, cell lines were co-cultivated with human fatty tissue (natural lipid source) in order to detect the amount of lipid droplets inside the different cell lines.

2.1. Supervised Research: Selecting Procedure for Lipid Droplet-Associated Genes

To identify lipid metabolism and lipid droplet-associated factors in breast cancer, a literature search was performed in the PubMed database related to LD-associated proteins (last search date: July 2022, Supplement S1). The publications with the keyword's lipid droplet-associated protein and their coded genes and the category review were collected. All references including human breast cancer cell lines and human cancer samples (for comparative purposes) were used for further studies. There was no restriction on the

publication period. The retrieved and selected factors were described to localize lipid droplets, including factors on contact sites for other organelles, such as the cell membrane, mitochondria, and endoplasmic reticulum.

2.2. Bioinformatics Design

For gene expression profiling, metastatic-stage expression (from I to IV) and overall survival (OS) analyses were performed by bioinformatics analysis on the GEPIA (gene-expression-profiling interactive analysis) platform (gepia.cancer-pku.cn, accessed on 20 June 2024) [25]. GEPIA is an online analysis tool for processing high-throughput RNA sequencing expression data of human cancer and normal samples based on the Cancer Genome Atlas (TCGA, portal.gdc.cancer.gov, accessed on 20 June 2024) and the Genotype-Tissue Expression (GTEx, www.gtexportal.org, accessed on 20 June 2024) databases. Employing the GEPIA platform, 1085 breast cancer samples and 291 healthy breast tissue samples were analyzed. In addition, dot maps of selected genes were generated. Furthermore, the GEPIA differential analysis module was used to analyze breast cancer gene-expression profiles, paired normal samples, and screen differentially expressed genes (DEGs) between tumor and normal tissues.

2.3. Unsupervised Research: Statistical Analysis

Statistical analysis was performed through the plug-in units of GEPIA. Analysis of variance (ANOVA) was performed and the Limma package plug-in was used for screening DEGs. The data analysis function of the Limma package is for the construction of linear models and differential expression for RNA-sequencing data. Genes with log2 (fold change) >1 or <–1, and a p-value < 0.05 were considered as DEG. p-values were calculated as false discovery rate (FDR)-adjusted p-values. The expression of the genes, and log2 (TPM + 1) for log-scale, were also applied to the pathological stages to understand whether the genes change among the metastatic stages. Depending on F statistics results and F-value > 2.5, the genes were also categorized according to whether they were pathological factors. DEGs were analyzed in more detail regrading overall survival (OS) on the GEPIA platform, which extracts the data from TCGA. Median expression was used as the threshold between high-expression and low-expression cohorts. OS analysis was performed using the Kaplan–Meier survival plots tool in the GEPIA platform. Via the log-rank test, log-rank p-values, hazard ratios (HRs), and Cox p-values were obtained. Univariate and multivariate Cox regression analysis was carried out via the Cox Proportional Hazards (CoxPH) function in R. $p < 0.05$ was considered as statistically significant. The activities of target genes in cancer and normal samples were shown under the heading expression, compared with each other, and then used in tables and figures according to their expression (over-express (OE) and under-express (UE)).

2.4. Cell Culture Experiments

The investigated human cell lines used in this study were MCF-10A, MDA-MB 231 and MDA-MB 346 (ATCC (American Type Culture Collection), www.atcc.org, accessed on 20 June 2024), which are well-established and representative breast cancer model systems [26]. MCF-10A is a human mammary non-tumorigenic epithelial cell line, which is widely used for in vitro studies of normal breast cancer function and transformation. MDA-MB-436 (derived from the metastatic site) and MDA-MB-231 (highly aggressive, and derived from the adenocarcinoma) are breast carcinoma cell lines with a mesenchymal-like phenotype, both being triple-negative breast cancer cell lines. All cell lines described in this paper were used with a passage number lower than 10, to ensure the same phenotypic properties as provided by the vendor.

The MCF-10A cells were cultured in a cell culture flask using a 1:1 mixture of Dulbecco's Modified Eagle's Medium (DMEM, Biochrom, with 4500 mg/L glucose, L-glutamine) and Ham's F12 medium (Biochrom, with L-glutamine) supplemented with 5% Horse Serum (HS), 20 ng/mL epidermal growth factor (EGF, Sigma-Aldrich, Taufkirchen, Germany),

10 µg/mL Insulin (Sigma-Aldrich), 100 ng/mL Cholera Toxin (Sigma-Aldrich), 500 ng/mL Hydrocortisone (Sigma-Aldrich) and 1% 10,000 U/mL penicillin/streptomycin (Biochrom). MDA-MB-436 and MDA-MB-231 cells were cultured in DMEM (Biochrom, with 4500 mg/L glucose, L-glutamine, without sodium pyruvate) supplemented with 10% fetal calf serum FCS (Biochrom) and 1% 10,000 U/mL penicillin/streptomycin (Biochrom).

During incubation, all cell lines were maintained at 37 °C and a CO_2 concentration of 5%. During the passaging step, adherent cells were detached with 1ml Trypsin, re-suspended in 4 mL medium and centrifuged at 100× *g*. Afterwards, the excess medium was aspirated and the cell pellet re-suspended with 900 µL medium. One cell suspension for every cell line was then transferred into an Eppendorf tube for subsequent lipid extraction. We did not try to isolate the LD, but relied exclusively on the analysis of the total extracts because the isolation of LD is time-consuming and would make high-throughput analysis much more difficult.

2.5. Lipid Extraction from Cell Lines

All three cell lines were extracted according to Folch [24], with slight modifications. First, three-times 100 µL of the cell suspension were transferred into Eppendorf tubes containing glass inserts. After adding 132 µL ice-cold methanol (BioSolve, Valkenswaard, The Netherlands) containing 0.05% butylated hydroxytoluene (BHT, Merck KGaA, Darmstadt, Germany) to each cell suspension, the samples were gently mixed for 10 min (600 rpm, 22 °C). Afterwards, 264 µL chloroform (Merck) containing 0.05% BHT was added to each sample, and the solutions were remixed for 60 min (600 rpm, 22 °C). Next, the samples were centrifuged (10 min, 12,000 rpm, 22 °C), and the lower phase of each replicate was transferred into a new glass vial using a Hamilton syringe. The upper phase was then extracted again with 132 µL chloroform for 30 min (600 rpm, 22 °C). After the sample was centrifuged once again (10 min, 12,000 rpm, 22 °C), the lower phases were combined in the glass insert, evaporated to dryness, and dissolved in 50 µL chloroform for further analysis.

2.6. High-Performance Thin-Layer Chromatography (HPTLC)

The extracted cell lines (n = 3 extractions from each cell line) were separated twice by normal phase HPTLC (HPTLC silica gel 60 MS-grade glass plates, 20 × 10 cm, Merck Millipore, Darmstadt, Germany) using two different solvent systems to separate either polar phospholipid classes or apolar lipids such as triacylglycerols and cholesteryl esters. Using a Linomat 5 (CAMAG, Berlin, Germany) combined with a Hamilton syringe, 1 µL of specific calibration mixture (concentration was 1 mg/mL) and 10 µL of each sample were applied to the HPTLC plate with 0.5 cm space between the spots and 1.5 cm from the bottom. The plates were developed in commercially available vertical TLC chambers (CAMAG, Switzerland) with chamber saturation, using either chloroform/ethanol/water/triethylamine (30/35/7/35, $v/v/v/v$) solvent mixture for the separation of phospholipid classes [27] or heptane/diethylether/acetic acid (40/10/0.5, $v/v/v$) to separate apolar lipids [28]. The HPTLC runs were performed at room temperature (22 ± 2 °C), 50 ± 5% relative humidity and a run time of about 60 min or 20 min, respectively. The total length of the run was about 8 cm. The developed TLC plate was dried in a stream of air. The analytes were visualized by dipping the plate into a primuline solution (Direct Yellow 59, c = 200 mg/L in acetone/water (8/2, v/v)). Upon irradiation with UV light (366 nm), analytes became detectable as violet spots which were scanned by a video densitometric device (Biostep GmbH, Jahnsdorf, Germany).

2.7. Electrospray Mass Spectrometry (ESI MS)

The visualized spots were marked with a pencil and analyzed by mass spectrometry. Selected spots of interest were directly eluted from the TLC plate using the Plate Express™ TLC plate reader (Advion, Ithaca, NY, USA) with methanol as solvent and subsequently analyzed by electrospray ionization mass spectrometry (ESI-MS) with an Amazon SL ion trap mass spectrometer (Bruker Daltonics, Bremen, Germany). Source parameters were

set to mass range mode, enhanced resolution; capillary voltage, 4500 V; end plate offset, 500 V; nebulizer (nitrogen), 70 psi; dry gas, 12 L/min; dry temperature, 200 °C. Data acquisition and analysis were performed using the Bruker software tools "TrapControl" and "DataAnalysis", respectively. Each lipid was identified manually according to its specific mass-to-charge (*m/z*) value. Results were verified by using the LIPID MAPS® database (The LIPID MAPS® Lipidomics Gateway, www.lipidmaps.org, accessed 3 April 2023).

Box plots for phosphatidylcholine spots, as one selected example, were generated with GraphPad Prism 8.4.3 (GraphPad Software, San Diego, CA, USA). Statistical significance was determined using a two-way ANOVA with Tukey's multiple comparisons test with alpha = 0.05. The test includes 14 rows (according to 14 PC species) and 3 columns (MCF-10A, MDA-MB-231 or MDA-MB-436), which were analyzed individually. The adjusted *p*-values were declared as follows: *, p value < 0.05; **, p-value < 0.01; ***, p-value < 0.001; ****, p-value < 0.0001.

2.8. Co-Culture Experiments of Cell Lines and Adipose Tissue

For co-culture experiments, all cell lines were seeded in 6 wells with 2 mL of their corresponding medium and co-cultured with 50 mg of human primary adipose tissue for different time points (see results). This was performed to mimic the physiological conditions of cancer growth. All adipose tissue samples were collected during laparoscopic abdominal surgery as described previously [29] in the context of the Leipzig obesity biobank and a two-step bariatric surgery approach as described in [30]. The study was approved by the ethics committee of the University of Leipzig (approval number: 159-12-21052012). The study design follows the Declaration of Helsinki, and all tissue donors gave written informed consent prior to participation in the study. The adipose tissue acted as donor of physiological concentrations of lipids into the medium and, thus, for the cell lines in co-culture. The adipose tissue pieces were placed in a 6-well insert (Greiner Bio-One, Art-Nr. 657610) and cultured with 500 µL of medium composed of DMEM with sodium pyruvate and L-glutamine (Capricorn scientific, DMEM-HPA), 10% FCS (Biochrom) and 1% 10,000 U/mL penicillin/streptomycin (Biochrom). The inserts were placed into the 6 wells, physically separating the adipose tissue and cell lines via a semipermeable membrane with a pore size of 1 µm. No cells passed the membranes.

2.9. Microscopy of the Lipid Droplets in the Co-Cultured Cell Lines

All cell co-culture images were recorded using an inverted Zeiss Axio Observer Z1 (Oberkochen, Germany), equipped with a Yokogawa CSU-X1A 5000 spinning disk confocal scanning unit, Hamamatsu Orca Flash 4.0 camera. The observation chamber was equilibrated to 37 °C and supplemented with 5% CO_2. For imaging, all cell lines were fixed with 4% Paraformaldehyde (PFA) followed by permeabilization in 0.1% Triton X-100 (Sigma Aldrich) in phosphate-buffered saline (PBS) for 10 min at room temperature. Subsequently, they were blocked with 1% bovine serum albumin in PBS for 10 min referring to [31]. The actin filaments were stained with SiR-Actin (Spirochrome, SC001), the nuclei with SPY-DNA555 (Spirochrome, SC201) and the lipid droplets with LipidTox Green (InvitrogenTM, H34475, Darmstadt, Germany).

3. Results and Discussion

Bioinformatic analysis of RNA-seq databases from both healthy and breast-cancer patients was employed to pinpoint the LD-related differentially expressed genes. Subsequently, experimental assessment of the lipid profiles across various cell lines was carried out using chromatographic and mass spectrometric techniques (see Experimental lipid analysis section). Finally, confocal fluorescence microscopy was used to observe different cell lines cultivated with human fatty tissue, enabling the assessment of lipid droplet quantity and the respective size.

3.1. Selection of Lipid Metabolism and Lipid Droplet-Associated Genes for the Bioinformatics and Cell Culture Analysis

For the selection of the lipid-related genes in breast cancer, supervised and unsupervised selection methods were used. After the supervised selection, following the literature search and analysis using the "Pubmed.gov" database, 143 genes were retrieved as LD-associated factors in breast cancer. The selection criteria consisted of both those genes directly implicated as LD-related genes and those localized on contact sites of LD with other organelles. Although Perilipin family members, which cover the LD, constitute the majority of publications, all retrieved genes and their functions are highly related to lipid metabolism and LD in breast cancer (Supplement S1). This is the main reason why another focus was on the evaluation of potential changes in the lipid compositions.

3.2. Significantly Altered Lipid Droplet-Associated Genes in Breast Cancer Patients

The RNA-seq expression data of the identified 143 genes were obtained from the lipid metabolism in 1085 human breast cancer tissue and 291 healthy breast tissue (human) samples. From the 143 genes applied to the GEPIA platform, 48 genes were identified as differentially expressed genes (DEGs) in breast cancer compared to normal breast tissues. While only *SQLE*, *FADS2*, and *MUC1* were over-expressed (OE), 45 genes (*ACADL*, *ACADS*, *ACSL1*, *ACSL4*, *AGPAT2*, *AKR1C1*, *ANGPTL8*, *C19orf80*, *APOB*, *AQP7*, *CAV1*, *CAV2*, *CAVIN1*, *CD133*, *CD36*, *CDCP2*, *CES1*, *CHKB*, *CIDEA*, *CIDEB*, *CIDEC*, *DGAT2*, *FABP4*, *FABP5*, *FABP7*, *FADS3*, *FOXO1*, *HSD17B11*, *HSD17B13*, *LIPD*, *LIPE*, *LPCAT2*, *LPL*, *MGLL*, *PEMT*, *PLA2G2A*, *PLA2G4A*, *PLA2G5*, *PLIN1*, *PLIN2*, *PLIN4*, *PNPLA2*, *PTGS2*, *SREBPF1*, and *CEBPA*) were identified as under-expressed (UE) in breast cancer tissue. For further details, see Supplement S2.

3.3. The Relation between Overall Survival Analysis of Lipid-Associated Genes and Their Expression in Breast Cancer Patients

The patient overall survival (OS) analysis of 143 DEGs was performed using the GEPIA platform. Table 1 summarizes the 28 genes with the lowest OS *p*-values (sorted from low to high). The results revealed that one over-expressed (*SQLE*) and five under-expressed genes (*FABP7*, *SAA4*, *CHKB*, *RBP4*, and *PLA2G4A*) were significantly associated with a decrease in OS (Table 1, column 5, highlighted as UE/S or OE/S). Although 48 genes were identified as DEGs, it did not mean that they were associated with a decrease in OS. Interestingly, 28 genes were confirmed by the above analysis as prognostic factors and significantly effective in breast cancer as lipid droplet-associated genes. From these genes in breast cancer patients, only 6, namely *FABP7* (UE, OS *p*-value: 0.0006), *CHKB* (UE, OS *p*-value: 0.02), *PLA2G4A* (UE, OS *p*-value: 0.05), *SAA4* (UE, OS *p*-value: 0.01), *RBP4* (UE, OS *p*-value: 0.02) and *SQLE* (OE, OS *p*-value: 0.041) showed both statistically significant changes in the OS HR and the expression (Table 1, columns 4 and 5). Although the OS *p*-values of the other 23 genes were significantly low, their expression did not change significantly and they are thus not suitable as prognostic factors. Thus, changes in the expression do not necessarily render a gene a prognostic factor, which is also important regarding the experimental lipid analysis data (vide infra). Although this would be extremely time-consuming, the determination of the related enzyme activities would provide some very useful information.

3.4. Significantly Changed Genes between Metastatic Transitions

Lipid-related genes were also examined as to whether they were effective in the cancerous transition, which includes four main metastatic stages, from I to IV. According to The Cancer Genome Atlas (TCGA), breast cancer stages are categorized as stage I–IV [32,33]. We adopted this categorization, providing further information regarding this classification in Section 3.8, below. With this analysis, the genes were analyzed in three different ways, including those with expression changes, those with OS, and those with significant changes between metastatic stages (Table 2). F statistic was used to determine if the mean values

between metastatic stage populations are significantly different. According to the F value of the 26 genes, *ACADS*, *AQP7*, *CAV1*, *CIDEA*, *CIDEC*, *CPA4*, *DGAT1*, *ELOVL5*, *FABP4*, *FABP6*, *FABP7*, *FADS6*, *FITM1*, *FITM2*, *HSD17B11*, *LIPE*, *MTTP*, *OSBPL2*, *PLA2G3*, *PLA2G4D*, *PLIN1*, *PLIN4*, *PNPLA2*, *PTGS2*, *SELE*, and *SELP* were identified as effective genes among metastatic stages. Among these 26 identified genes, 13 were significantly under-expressed (UE/S) and are highlighted in Table 2 (column 4, abbreviated bold in UE/S). Only one of these genes, *FABP7*, was significantly low in its prognostic effect (OS *p*-value). With this analysis, it can be stated that these genes are both tumor effective and play crucial roles in the aggressiveness of cancer. This confirms former data obtained by Chang and Xing [34].

Table 1. The lowest overall survival of the genes: 28 genes with the lowest overall survival (OS) *p*-values, sorted from low to high. (OS *p*-value = overall survival *p*-value, OS HR = overall survival hazard ratio, F-value = F statistics calculation value, metastatic *p*-Value = F statistics *p*-value, OE = over-expressed, UE = under-expressed, UE/S or OE/S = significantly over- or under-expressed).

Gene Name	Description	OS *p*-Value	OS HR	Expression	F-Value	Metastatic *p*-Value
FABP7	Fatty Acid Binding Protein 7	0.0006	0.57	UE/S	3.310	0.0100
LAMP2	Lysosomal-Associated Protein	0.0020	1.70	Same	0.513	0.7200
ELOVL2	Fatty Acid Elongase 2	0.0030	0.62	OE	0.660	0.6100
APOBEC3G	Apolipoprotein mRNA editing enzyme	0.0040	0.62	UE	2.000	0.0920
OSBPL2	Oxysterol-Binding Protein	0.0070	1.60	OS	2.730	0.0200
PLA2G10	Phospholipase A_2 Group X	0.0070	0.64	OS	0.600	0.6600
PLA2G1B	Phospholipase A_2 Group IB	0.0090	0.65	Same	1.590	0.1700
FOXO3	Forkhead Box O3	0.0090	1.50	UE	0.669	0.6140
CPA4	Carboxypeptidase A4	0.0100	1.50	UE	2.300	0.0500
ELOVL1	Fatty Acid Elongase 1	0.0100	1.50	OE	0.811	0.5100
FKBP5	FKBP Prolyl Isomerase 5	0.0100	0.68	UE	0.300	0.8700
PLIN5	Perilipin 5	0.0100	0.65	UE	0.811	0.5100
SAA4	Serum Amyloid A4	0.0100	0.68	UE/S	1.270	0.2000
TMEM229B	Transmembrane Protein 229B	0.0100	0.66	OE	1.500	0.2000
SELL	Selectin L	0.0160	0.67	Same	1.300	0.2000
LSS	Lanosterol Synthase	0.0170	1.50	UE	0.660	0.6100
CHKB	Choline Kinase Beta	0.0200	0.68	UE/S	1.040	0.3800
CXCR6	C-X-C Motif Chemokine Receptor 6	0.0200	0.68	Same	1.050	0.3800
LPCAT1	Lysophosphatidylcholine Acyltransferase	0.0200	1.50	OE	0.300	0.8200
PLA2G15	Phospholipase A2 Group XV	0.0200	1.40	OE	2.030	0.0800
RBP4	Retinol Binding Protein 4	0.0200	0.70	UE/S	3.790	0.0045
DGAT1	Diacylglycerol O-Acyltransferase 1	0.0280	1.40	Same	2.800	0.0200
CHKA	Choline Kinase Alfa	0.0400	1.40	UE	0.770	0.5400
FADS6	Fatty Acid Desaturase 6	0.0400	0.71	Same	2.800	0.0200
LRGUK	Leucine-Rich Repeats and Guanylate Kinase	0.0400	0.71	OE	1.260	0.2800
SQLE	Squalene Epoxidase	0.0410	1.40	OE/S	2.160	0.0700
PIM2	Pim-2 Proto-Oncogene	0.0500	0.73	OE	1.840	0.1100
PLA2G4A	Phospholipase A2 Group IVA	0.0500	0.73	UE/S	2.160	0.0700

Table 2. Gene list sorted by F-Value: 26 genes with the highest F-value (after F statistics) and the lowest metastatic *p*-values. Bold values show the statistically significant ones. (OS *p*-value = overall survival *p*-value, OS HR = overall survival hazard ratio, F-value = F statistics calculation value, Metastatic *p*-value = F statistics *p*-value, OE = over-expressed, UE = under-expressed, UE/S or OE/S = significantly over- or under-expressed).

Gene Name	Description	OS *p*-Value	Express.	F-Value	Metastatic *p*-Value
SELP	Selectin P	0.5500	UE	7.25	0.0100
PLIN1	Perilipin1	0.3700	UE/S	5.00	0.0005
FABP4	Fatty-Acid-Binding Protein	0.2400	UE/S	5.11	0.0004
CIDEC	Cell Death-Inducing DFFA-Like Effector C	0.4900	UE/S	4.47	0.0010
PTGS2	Prostaglandin-Endoperoxide Synthase 2	0.3900	UE/S	4.45	0.0010
AQP7	Aquaporin 7	0.2900	UE/S	4.25	0.0020
SELE	Selectin E	0.5100	UE	4.09	0.0020
DGAT1	Diacylglycerol O-Acyltransferase 1	0.0270	Same	3.79	0.0040
CIDEA	Cell Death-Inducing DFFA-Like Effector A	0.1100	UE/S	3.59	0.0060
FITM1	Fat Storage-Inducing Transmembrane Protein 1	0.0710	UE	3.44	0.0080
LIPE	Lipase E, Hormone-Sensitive Type	0.7200	UE/S	3.44	0.0080
FABP7	Fatty-Acid-Binding Protein	0.0006	UE/S	3.31	0.0100
FITM2	Fat Storage-Inducing Transmembrane Protein 2	0.1100	UE	3.28	0.0100
PLIN4	Perilipin4	0.4200	UE/S	3.21	0.0100
CAV1	Caveolin 1	0.3400	UE/S	3.20	0.0100
ELOVL5	ELOVL Fatty Acid Elongase 5	0.3900	UE	3.01	0.0100
FADS6	Fatty Acid Desaturase 6	0.0400	Same	2.80	0.0200
ACADS	Acyl-CoA Dehydrogenase Short Chain	0.8900	UE/S	2.79	0.0200
OSBPL2	Oxysterol-Binding Protein-Like 2	0.0066	OE	2.73	0.0200
HSD17B11	Hydroxysteroid 17-Beta Dehydrogenase 11	0.2800	UE/S	2.70	0.0200
FABP6	Fatty-Acid-Binding Protein 6	0.3200	Same	2.58	0.0300
MTTP	Microsomal Triglyceride Transfer Protein	1.000	UE	2.56	0.0300
PLA2G4D	Phospholipase A2 Group IVD	0.4600	OE	2.54	0.0300
PLA2G3	Phospholipase A2 Group III	0.8800	UE	2.45	0.0400
CPA4	Carboxypeptidase A4	0.0150	UE	2.30	0.0500
PNPLA2	Patatin-Like Phospholipase Domain-Containing 2	0.100	UE/S	2.28	0.0500

3.5. An Outstanding Gene: FABP7

The most prominent gene among all the analyzed genes is *FABP7* (Fatty-Acid-Binding Protein). These proteins represent a family of transport proteins for fatty acids and other lipophilic substances such as eicosanoids and retinoids. They are assumed to facilitate the transfer of fatty acids between extra- and intracellular membranes, and thus are presumably involved in LD formation. *FABP7* has shown statistical significance in all criteria: as a prognostic factor (OS *p*-value = 0.0006) it is statistically low, with log2 = −1.307, which is an under-expression, and with an F-value of 3.31 among metastatic transition with a *p*-value of 0.01. Since no other gene showed significant features in all of these three analyses, this gene might be a potential biomarker for breast cancer (Figure 2). Although the expression *FABP7* is under-expressed in cancer samples compared to healthy samples in the GEPIA platform, it shows a different expression profile in other cancer types. When *FABP7* was examined using the cancer expression platform http://firebrowse.org (accessed 20 June

2024) (Supplement S6), it was seen that this gene showed a different expression profile depending on the cancer type. In addition, the gene expression also shows lower and higher expression in breast cancer subtypes and breast cancer-lineage subtypes (Supplement S7). In fact, although the gene expression is high in some breast cancer studies, *FABP7* is an unstable cancer-specific gene and can be considered as a biomarker [34].

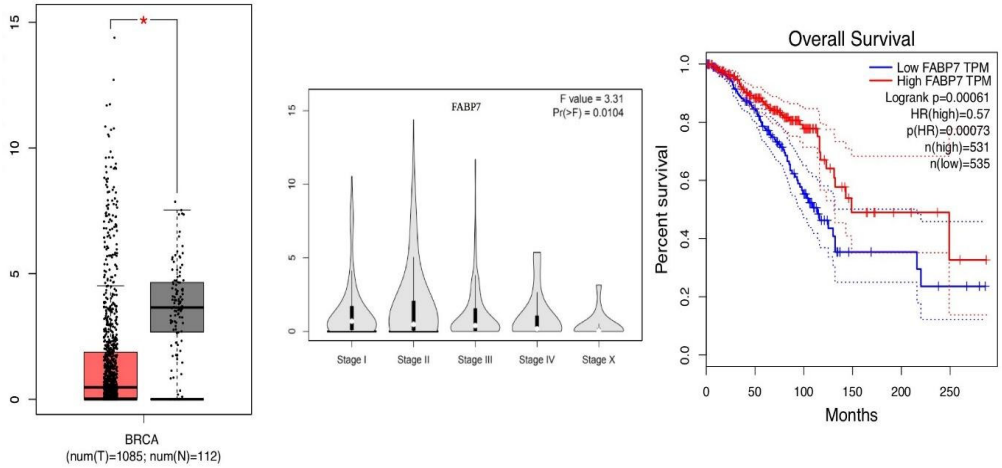

Figure 2. Expression Analysis of *FABP7*. Differential expression (**left**), metastatic transition stages (**middle**) and overall survival (OS, **right**) images of *FABP7*. (**Left**): the gene is drastically under-expressed in tumor samples (red box) compared to normal tissue (gray box), red star shows the differences is statistically significant. (**Middle**): there are significant alterations between the metastatic stages (Stage I–IV, Stage X means unknown) [30], which leads to the high F-value. (**Right**): the OS analysis indicates *FABP7* as a prognostic factor for breast cancer. The Y axis of BRCA and metastatic stages shows expression value which is calculated as log2(TPM + 1) for log-scale.

3.6. Both Overall Survival and Metastatic Transition Significant Genes

After completing our triple analysis, four genes (from Tables 1 and 2) were identified as statistically significant in OS and metastatic transition. The genes shown in Figure 3 are *DGAT1* (OS p = 0.027, HR: 1.4, F-value: 3.79); *OSBPL2* (p = 0.0066, HR: 1.6 F-value: 2.73); *CPA4* (p = 0.015, HR; 1.5, F-value: 2.3); and *FADS6* (p = 0.04, HR: 0.71, F-value: 2.80). Although expression of these genes does not show statistical significance between tumor and healthy states, they do demonstrate distinct expression patterns among the metastatic stages, with their OS results bearing statistical significance. Regardless of gene expression within the tumor samples (n = 1085), genes having a high F-value could be effective in metastatic transitions and play essential roles in the aggressiveness of cancer and could be prognostic factors that can affect the clinical outcome. This means that they may have a direct effect on the rapid progression of the disease and, ultimately, on the life span of the patients (Figure 3).

3.7. Overall Survival Analysis

According to OS analysis of 143 selected genes in breast cancer, 28 of them show statistically significant p-values of <0.05. *FABP7*, *LAMP2*, *ELOVL2*, *APOBEC3G*, *OSBPL2*, *PLA2G10*, *PLA2G1B*, *FOXO3*, and *CPA4* were identified as the nine genes with the lowest OS p-values of 0.0006, 0.002, 0.003, 0.004, 0.007, 0.0075, 0.009, 0.0095, and 0.01, respectively (Figure 4). The analysis results of all these genes were obtained as images and compared with each other. The other OS significant genes were also combined and compared as images (Supplement S3).

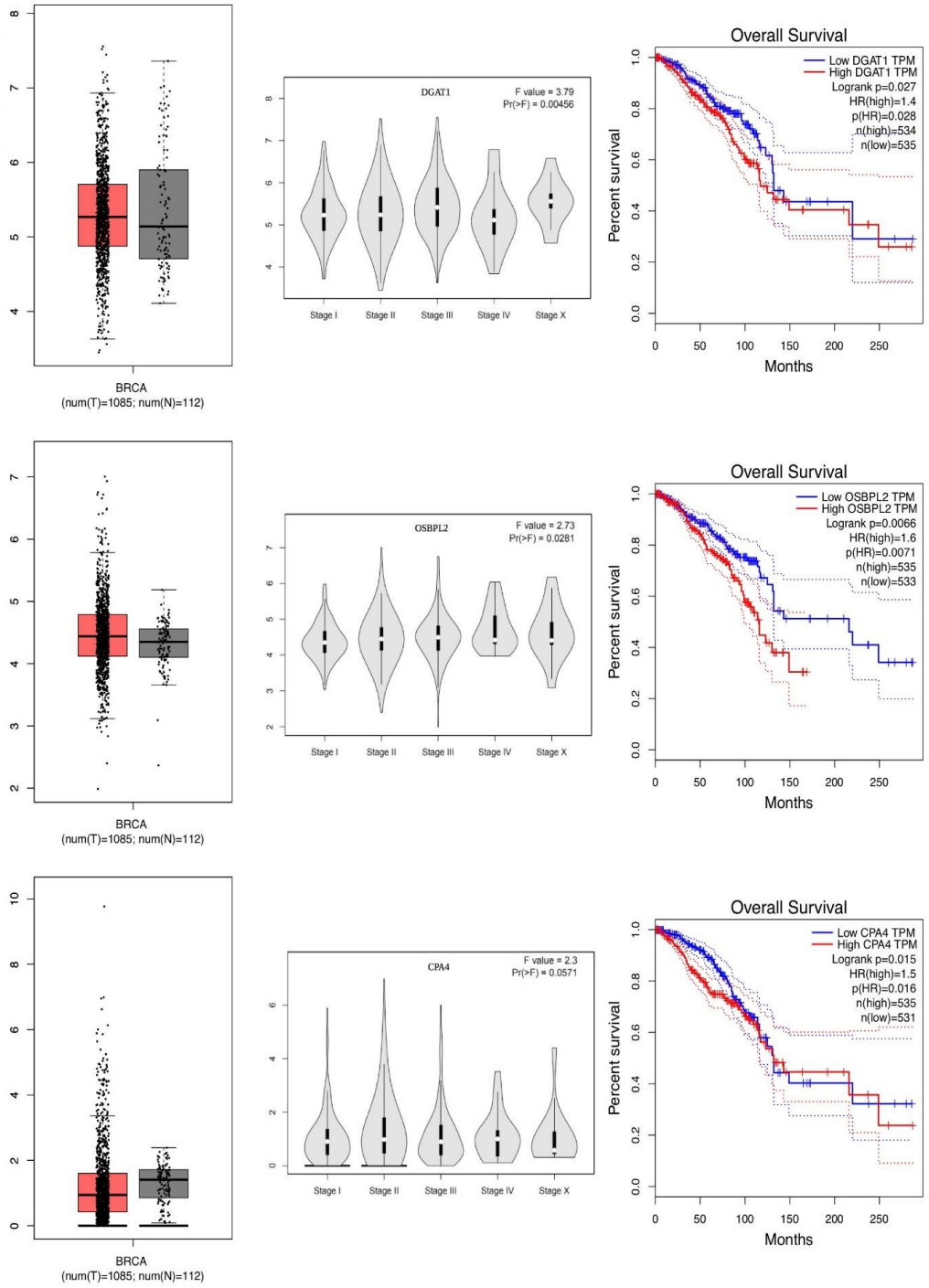

Figure 3. The other significantly-changed genes. Next to *FABP7*, three more genes are commonly significant in OS, HR, and F-value: *DGAT1* (first row), *OSBPL2* (second row) and *CPA4* (third row). The left figure compares the expression of genes between tumor (red box) and healthy (gray box) tissue. The middle figure shows the genes' effectiveness during metastatic transitions. The right figure is an OS analysis of the same genes and shows how they play a role in the long term. The Y axis of BRCA and metastatic stages shows expression value which is calculated as log2(TPM + 1) for log-scale.

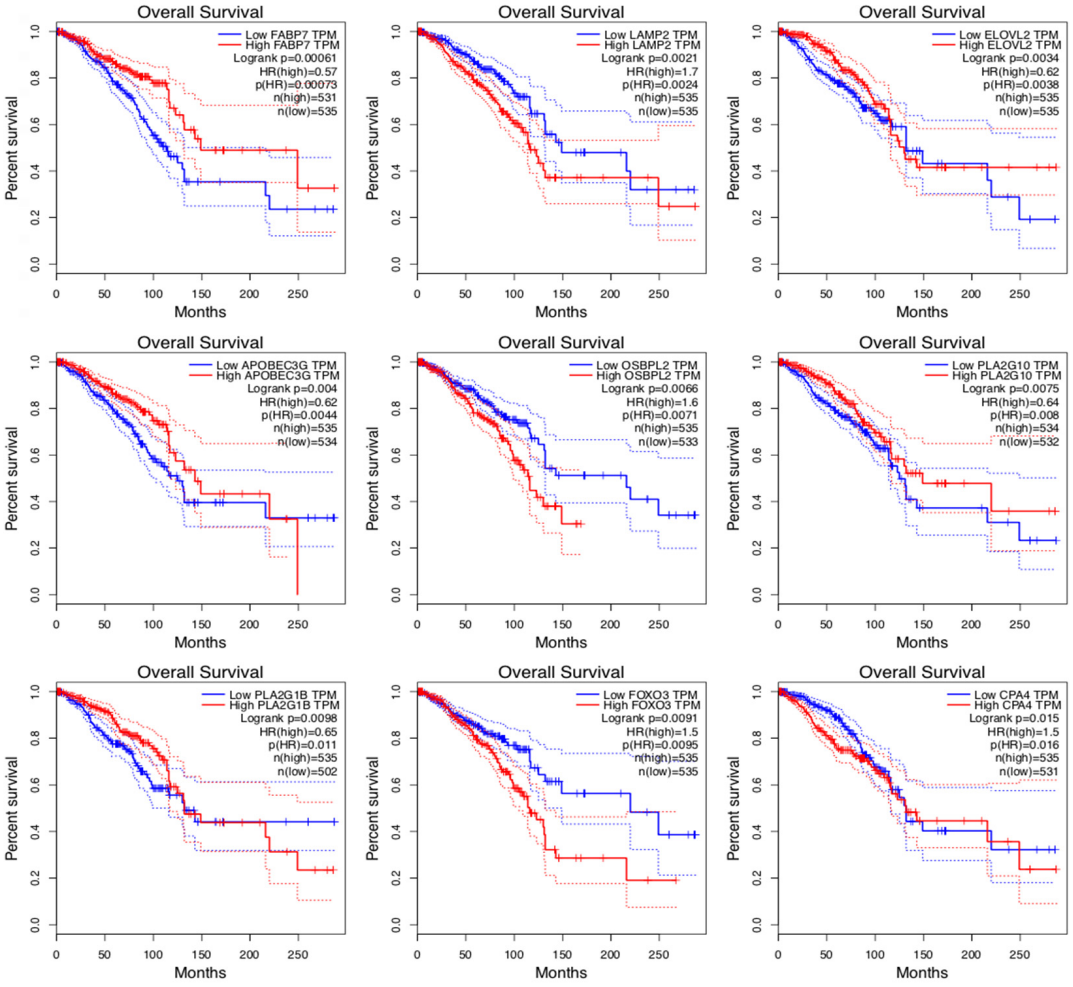

Figure 4. OS survival of nine genes with lowest OS *p*-values. Since each of these figures shows the overall survival analysis together with, in detail, Log-rank, HR (hazard ratio) and *p* (HR), the comparison of the data is straightforward.

The reason we used multiple analytical approaches at the same time was the fact that LD-related genes differ in cancer and normal tissues. In addition, we wanted to detect whether the expression of these genes differ (and fluctuate) in metastatic transitions. Finally, we wanted to see which genes were prognostic for OS. It turned out that some of our target genes were under- and some were over-expressed. Similarly, it became evident that, while some of the genes were active in metastatic stage transitions, there was no change in the expression of other ones. Thus, the changes according to the samples were not active in metastatic transitions. This led us to the conclusion that genes showing any change in expression do not play a role in metastases. Likewise, we found that those which did not show any difference in their expression or metastatic stages, had statistically prognostic features in OS analyses, depending on the GEPIA database.

3.8. Metastatic Stage Analysis of All the Genes

Among the 26 genes that were identified as significantly changed in metastatic stages of breast cancer, the following were shown to have the highest F-values: *SELP*, *PLIN1*, *FABP4*, *CIDEC*, *PTGS2*, *AQP7*, *SELE*, *DGAT1*, and *CIDEA* (F-values of 7.25, 5.0, 5.11, 4.47, 4.45, 4.25, 4.09,3.79, and 3.59, respectively) (Figure 5). F-values of the other genes were imaged and compared (Supplement S4). In addition, the target genes were applied to Disease Free Survival analysis. As a result, *ELOVL2*, *FKBP5*, *LRGUK*, *PIM2*, *PLIN5*, *SELL*, and *TMEME229B* showed the lowest *p*-value and *CPA4*, *LAMP2*, *LPCAT1*, and *PLA2G15* the highest HR value, respectively (Supplement S5).

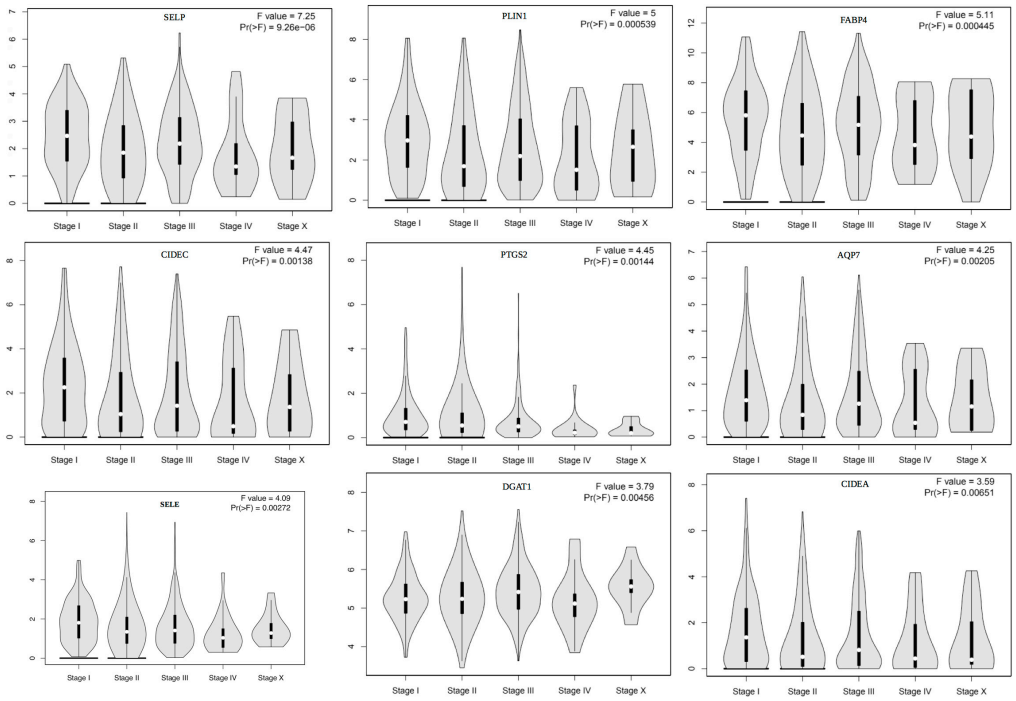

Figure 5. Nine genes with the highest F-values. These figures show differentially expressed genes (DEGs) between metastatic stages. The differences are calculated as F Statistics and presented by F-value and *p*-value of F-value. Combining these images enables the visualization of how the genes' expression changes between different stages.

3.9. Unsupervised DEGs in Breast Cancer Tissue

As one result of the unsupervised DEG analysis on the GEPIA platform, 1418 over-expressed and 2138 under-expressed genes were identified in breast cancer based on GRCh38.p2 (NCBI) data. According to the DEG in breast cancer, the fold change (log2) of gene expression was sorted by using the gepia.cancer-pku.cn link. Based on sorting the genes, the lowest 20 under-expressed genes were identified and 17 of the 20 genes were related to lipid droplets and lipid mechanism (Table 3). *ADH1B* and *FABP4* are the two most under-expressed genes, with fold changing −6.67 and −6.62 log2 base, respectively (Table 3, column 5). Metastatic stage expression and OS analysis of these genes were added to the results, which clarified the comparison and evaluation (Table 3, columns 6–8). The changes in tumor/normal comparisons of these 20 genes and between metastatic stages showed us how effective genes are. In addition, 17 genes, except *RBP4*, *LEP*, and *GPX3*, statistically change between metastatic stages, indicating that these genes play an active role in tumor formation and metastatic aggressiveness. In a healthy breast cell, the expression of the genes is higher than in breast cancer cells. While the LD sizes and radii are increasing in breast cancer cell tissue, expression of the genes, which control the mechanism of lipid, become under-expressed. It is reasonable to assume that the lipid metabolism and LD formation cannot be sufficiently controlled by the genes which are responsible for them, as compared with healthy breast cells. This indicates that there is a so far unknown LD mechanism in cancer.

Table 3. Gene list sorted by fold differences. The lowest-expressed 20 genes in Breast Cancer depending on sorting of the fold changes of gene expression in breast cancer; from the lowest-expressed genes compared with normal expression in the human breast.

Gene Name	Description	Tumor	Normal	Fold	F Statistics F-Value	Metastatic Stages *p*-Value	OS *p*-Value
ADH1B	Alcohol Dehydrogenase	4.62	570.70	**−6.67**	5.72	0.0001	0.82
FABP4	Fatty Acid binding	30.29	3082.96	**−6.62**	5.11	0.0004	0.82
CIDEC	Lipid Droplet Formation	1.35	204.92	**−6.45**	4.47	0.0010	0.89
PLIN1	Lipid Droplet	3.23	274.45	**−6.03**	5.00	0.0005	0.86
GPD1	Catalyzing lipid	1.94	150.75	**−5.69**	3.50	0.0030	0.79
ADIPOQ	Adiponectin	1.78	135.23	**−5.62**	4.09	0.0020	0.81
RBP4	Lipocalin	3.47	203.23	**−5.51**	1.89	0.1100	0.70
PLIN4	Lipid Droplet	2.82	167.73	**−5.47**	3.21	0.0100	0.88
CD300LG	Nepmucin	0.36	55.48	**−5.38**	3.71	0.0050	0.98
AQP7	Aquaporin adipose	0.98	80.56	**−5.36**	4.25	0.0020	0.84
HSPB6	Heat Shock Protein	6.52	298.27	**−5.32**	5.83	0.0001	0.92
BTNL9	Exter.Pla.Memb	1.60	95.04	**−5.21**	3.68	0.0050	1.10
CFD	Peptidase	14.95	571.22	**−5.17**	2.71	0.0200	0.91
LEP	Leptin	0.18	39.49	**−5.10**	1.88	0.1100	0.80
GPX3	Gluthatione Perox.	32.81	1132.11	**−5.07**	1.98	0.0900	0.99
CIDEA	Lipid Droplet Formation	0.62	52.74	**−5.05**	3.59	0.0060	0.77
CA4	Anchored membrane isozyme	0.11	35.12	**−5.02**	2.93	0.0200	0.94
TUSC5	Plasma membrane protein	0.43	41.68	**−4.9**	2.85	0.0200	0.78
TIMP4	Peptidase	1.08	58.56	**−4.84**	2.68	0.0300	0.87
CLDN5	Tight junction	5.64	172.78	**−4.71**	5.91	0.0001	0.91

3.10. Lipid Profile by Thin-Layer Chromatography Coupled with Mass Spectrometry

Next, we analyzed the lipid profile of different cell lines using chromatographic and mass spectrometric techniques in a pilot study. The determination of the complete sample of lipidome was not the aim of this study. This is the reason why only selected lipid fingerprints and physical—not biological—replicates were evaluated. The cell line MCF-10A, as a non-tumorigenic epithelial cell line, was used as a reference sample. In addition, the cell lines MDA-MB436 and MDA-MB-231 are both established breast cancer cell lines and described as metastatic mesenchymal and highly aggressive mesenchymal, respectively (see Section 2).

We first started with the general lipid profile of lipid extracts (n = 3 each) from all three cell lines, using high performance thin-layer chromatography (HPTLC) to separate polar lipids (Figure 6). The developed HPTLC plate indicates a complex lipid profile (Figure 6A) with many polar lipids such as phosphatidylcholine (PC), —-ethanolamine (PE), —-inositol (PI), —-glycerol (PG), lyso-PC (LPC), sphingomyelin (SM) and free fatty acids (FFAs) as a comparably apolar lipid class. The other apolar lipids (cholesteryl ester (CE), free cholesterol (FC), triacylglycerols (TAGs), diacylglycerols (DAGs) and monoacylglycerols (MAGs)) could be found as a non-resolved band in the solvent front. It is obvious that there are no major changes between the spot intensities within one lipid class, although the spots from MDA-MB-231 are a bit less intense. Since we were interested to analyze the lipid spots with mass spectrometry (after re-elution from the silica gel) to obtain a deeper look into the

lipid fingerprint pattern, we used primuline as a non-destructive dye. Primuline is known to bind to the apolar fatty acyl residues of lipids but the resulting fluorescence intensity additionally depends on the polar headgroup of the lipids [35]. This makes quantitative data analysis (without many internal standards) extremely challenging. As we have already stated, our intension was just to present some lipid fingerprints—not a comprehensive lipidomic study, so far. Nevertheless, even the primuline dye allows for densitometric analysis, leading to the relative distribution of lipid classes, which is summarized in Figure 6B. From the three pie charts, it is obvious that the relative distribution is the same. Thus, it can be summarized that the total lipid fingerprint (excluding CE, FC and TAG) is nearly identical for all cell lines, independent whether they represent non-metastatic (MCF-10A) or metastatic (MDA-MB 231 and 436) cells.

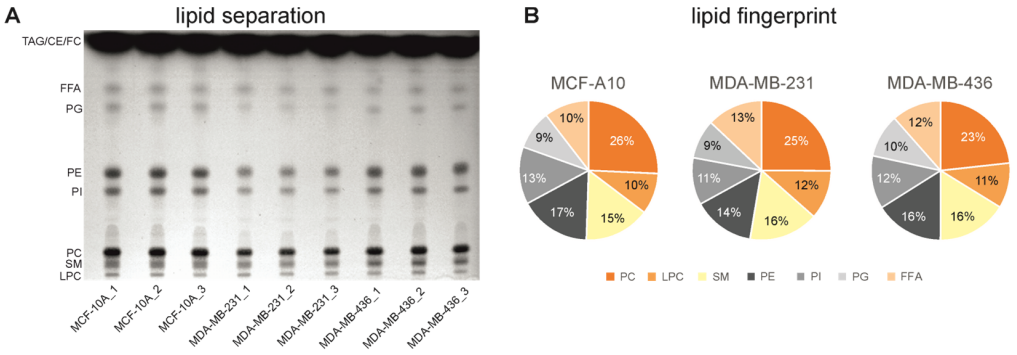

Figure 6. Lipid separation and lipid fingerprint. (**A**) Separation of polar lipids by high-performance thin-layer chromatography (HPTLC) and visualization under UV light (366 nm) after primuline staining. (**B**) Relative lipid distribution of different cell lines using densitometry. Independent of the cell line, the overall lipid composition is very similar. Abbreviations: phosphatidylcholine (PC)—ethanolamine (PE)—inositol (PI)—glycerol (PG), lyso-PC (LPC), sphingomyelin (SM), free fatty acids (FFAs), cholesteryl ester (CE), free cholesterol (FC) and triacylglycerols (TAGs).

Since TLC alone does not allow the structural identification of individual lipids by their fatty acyl compositions, but only the characteristic headgroup, the cell lines were also analyzed by mass spectrometry using an automatic extraction device (Advion Plate Express, see Section 2 (Material and Methods)) coupled to an ESI-IT mass spectrometer. Due to the limited space, we only show the identified PC species (Figure 7) as one selected example. As a first result, it can be stated that the acyl chain length as well as the number of double bonds increases if the tumor character of the cells increases (Figure 7). For instance, PC 38:5, PC 38:4, PC 38:3, PC 40:6 and PC 40:5 are much more abundant in the tumorigenic cell lines compared to the control, although only PCs with 38 carbon atoms are significantly reduced (adjusted p-value < 0.05 marked with * and <0.01 with **). This is in line with the assumption that the fluidity and thus the fusiogenic ability of tumor cells is elevated by a higher double-bond content [36]. The more aggressive cell line MDA-MB-231 (Figure 7, light gray box plots) is characterized by the highest content of polyunsaturated fatty acids (PUFAs), which strengthens the hypothesis that more aggressive tumors possess a higher fluidity.

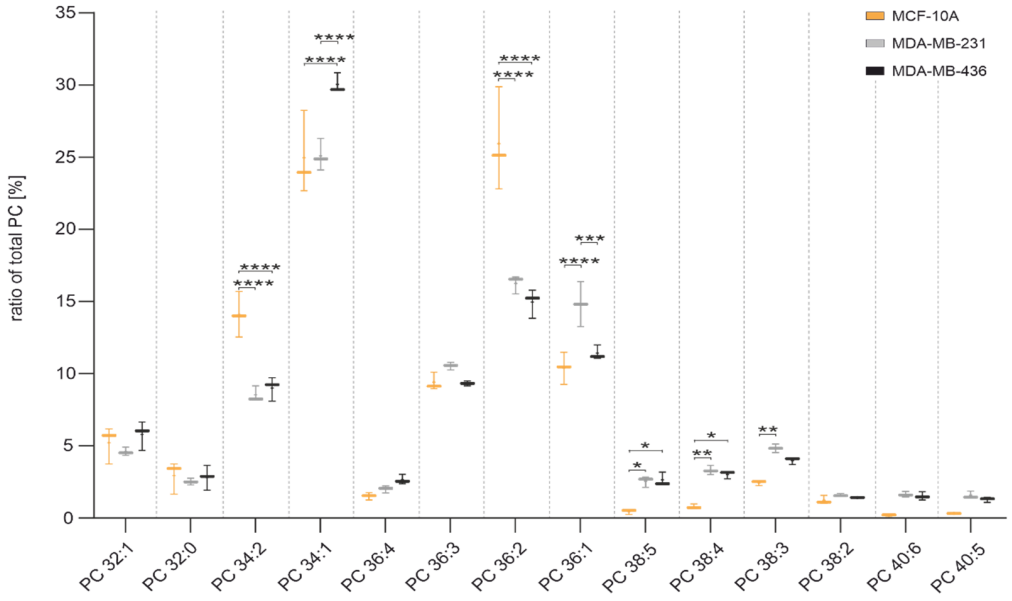

Figure 7. Relative intensities of identified PC species after HPTLC-ESI IT MS from different cell lines (n = 3). Spots of interest were released by direct elution using the Plate Express^{TM} TLC plate reader with methanol as the solvent. Most significant differences could be found between the control cell line (MCF-10A, yellow) and both tumorigenic cell lines MDA-MB-231 (gray) and MDA-MB-436 (black). Significances were classified using two-way ANOVA with Tukey's multiple comparisons test as follows: * p value < 0.05; ** p-value < 0.01; *** p-value < 0.001; **** p-value < 0.0001.

Details of the data given in Figure 7 remain to be elucidated. However, it is obvious that there are changes both to the double-bond content, as well as the chain length. This is in line with the shown increased polyunsaturated lipid profile in mesenchymal breast cancer cells in [37]. From the genomic database research, the gene *ELOVL2* (Table 1) is over-expressed in breast cancer and known to catalyze the synthesis of C20- and C22-*PUFA*, which are elevated in our investigated cancer cell lines (PC 40:6 and PC 40:5). Moreover, the *ELOVL2* gene shows a significant OS ratio (OS p-value 0.003), which means that patients suffering from breast cancer have a low OS. Thus, the link between *ELOVL2* and the *PUFA* content might be a future indicator for breast cancer. We will communicate this data in more detail in due course. A similar behavior could also be monitored in the case of the sphingomyelins. In this case it was obvious, too, that the chain length, particularly that of 24:0 (lignoceric acid) and 24:1 (nervonic acid) increases if the tumor character of the cells increases. For one specific protein, *ELOVL1*, which is a specific fatty acid elongase for the C24 sphingolipid synthesis [38], over-expression resulted after statistical analysis (Table 1). Thus, higher gene expression of *ELOVL1* might be one reason for the enhanced SM synthesis with C24 fatty acyl residues. In a nutshell, apparent differences can be observed if the PC and SM compositions of the different cells are compared. In particular, the chain lengths of the fatty acyl residues in the lipids are significantly increased under cancer conditions, which is in accordance with the over-expression of the two *ELOVL1* genes. Additionally, one specific gene, *PLA2G4A*, which encodes a phospholipase leading to the cleavage of the fatty acyl residue in *sn*2-position from the glycerol backbone of lipids is significantly under-expressed and shows a significant OS p-value (0.0500) (Table 3), leading to a low survival chance for the patient. Since *PLA2G4A* seems to hydrolyze particularly *sn*2-arachidonyl residues in membrane PL [39], leading to the corresponding LPL and free arachidonic acid as an important eicosanoid precursor, its under-expression should lead to higher moieties of PL-bound arachidonoyl residues. Accordingly, it is obvious from Figure 8 that only PC 36:4, PC 38:5, PC 38:4, PC 40:6 and PC 40:5 might contain arachidonic acid. All five PC species are elevated in cancerous cell lines. This supports the hypothesis that the under-expressed *PLA2G4A* gene leads to elevated arachidonic

acid concentrations in breast cancer. Nevertheless, further experiments to verify this hypothesis will be performed. Due to the significant under-expression of FABP7 in breast cancer tissue including a significant OS *p*-value (0.006), an F-value of 3.31 and a significant metastatic *p*-value (0.01), the gene might be an excellent prognostic factor for the early detection of breast cancer. According to [40], *FABP7* has a high binding affinity to n-3 polyunsaturated fatty acids such as α-linolenic acid (18:3), eicosapentanoic acid (20:5) and docosahexanoic acid (22:6), but also to the monounsaturated oleic acid (18:1). If the gene is under-expressed in breast cancer, the concentration of these specific fatty acids should be lower in comparison to the healthy controls. For now, the specific fatty acid distribution was not targeted, due to limited access to fragmentation experiments (MS/MS) using our TLC-ESI MS approach. Nevertheless, future experiments to monitor these fatty acids either as free fatty acids or as part of glycero(phospho)lipids are planned, using high-performance liquid chromatography (HPLC)-MS/MS in breast cancer tissue as well as breast cancer cell lines and comparing results to healthy control samples. These experiments will help to obtain deeper insights into the correlation of the FABP7 gene and lipid concentrations of specific FABP7-binding fatty acids in real tissue and/or blood samples.

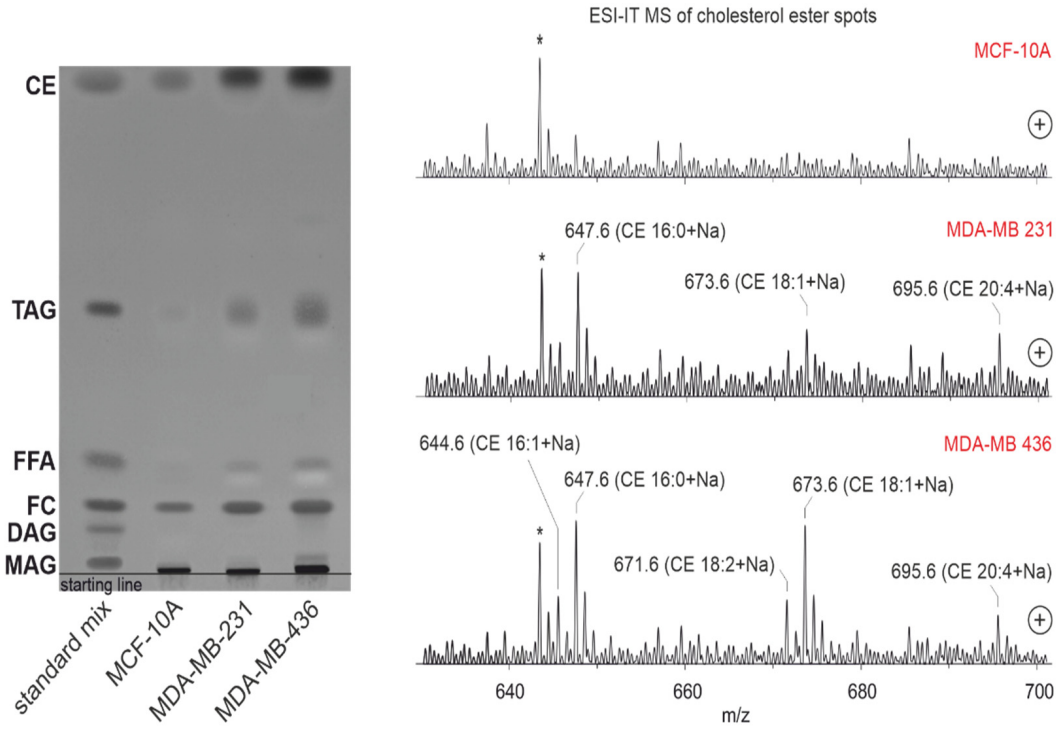

Figure 8. TLC image of separated apolar lipids of standard mixture and cellular extracts. MCF-10A as reference cell line and MDA-MB-231 and MDA-MB-436 as cancerous cell lines. Spot intensities of both cancer cell lines lead to the assumption of higher amounts of apolar lipids and thus to higher lipid droplet concentration. Although the spots could be clearly identified using the video densitometric device in all cell lines, the extraction process during the direct infusion ESI-IT MS leads to the loss of lipids, which makes the measurements difficult for low-abundance lipids. Thus, only cholesterol ester (CE) species in both MDA-MB cell lines could be identified, but not in the MCF-10A. Triacylglycerol (TAG) concentrations were under the detection limit as well. Background signals in the ESI-IT mass spectrum are marked with an asterisk (*). Abbreviations: monoacylglycerol (MAG), diacylglycerol (DAG), free cholesterol (FC), free fatty acid (FFA), triacylglycerol (TAG), cholesterol ester (CE).

To summarize the so far obtained results for polar PL in breast cancer cell lines and normal cells, only coarse correlations between genomic and lipidomic results could be found. This fact emphasizes that the exclusive consideration of changes in the genome

is a not very reliable approach, but additional experimental compositional data are also required (a similar conclusion, that gene expression data are not sufficient as a single signature, was also made by [41]). Additionally, while alterations in the protein levels often accompany changes in gene expression, the concentrations alone are not indicative of metabolic processes and the related changes. This reflects the aspect that enzymes are required to induce metabolic alterations. Therefore, the presence of an enzyme, i.e., the protein concentration, does not necessarily indicate an elevated enzyme activity. This important aspect of enzymatic activity will be considered separately in future reports.

The separation of apolar lipids by HPTLC was performed with another solvent system (see Material and Methods section), leading to the separation of monoacylglycerol (MAG), diacylglycerol (DAG), free cholesterol (FC), free fatty acid (FFA), triacylglycerol (TAG) and cholesterol ester (CE) species, as shown in Figure 8, for one replicate per cell line, as an example. The mass spectrometric analysis of the re-extracted spots allowed the detection of five CE species, but exclusively in the two cancer cell lines. The mass-to-charge ratios (*m/z*) of 645.6, 647.6, 671.6, 673.6 and 695.6 could be identified as $[M + Na]^+$ adducts of CE 16:1, CE 16:0, CE 18:2, CE 18:1 and CE 20:4, respectively. The CE concentration in MCF-10A was beyond the detection limit, since no CE species could be identified with ESI-IT MS after the extraction process. TAG identification was not possible due to the low concentrations, as it is commonly accepted in cell lines [42]. Future experiments with more sensitive and precise MS methods, as well as improved extraction methods, are in progress. Nevertheless, the spot intensity itself leads to the assumption of higher CE and TAG concentrations in cancer cell lines. Thus, the hypothesis of higher LD amounts in cancer could be confirmed via HPTLC. Nevertheless, further experiments using knock-down, knock-out or knock-in experiments with *FABP7* are necessary, and will be performed in the future.

3.11. Lipid Droplet Accumulation in Cell Lines

To check the physical presence of LD accumulation in cancerous cell lines, microscopic images from the MCF-10A cell line as a model for an epithelial cell and the MDA-MB-231 cell line, as a highly aggressive mesenchymal cell, were acquired. Our hypothesis was that there should be higher amounts of apolar lipids (such as CE and TAG from the experimental approach) in breast cancer cell lines, compared to the control cells of the same type, following co-cultivation with primary adipose tissue. To assess this, LDs were fluorescently labeled and quantified semi-quantitatively (Figure 9, left). The amount of lipid droplets (pseudo-colored in yellow) remained relatively unchanged for the MCF-10A cells. In contrast, for the MDA-MB-231 cells, both the amount and size of lipid droplets showed an increase following a 10-day co-culture with primary adipose tissue. In addition, the relative particle-size distribution of lipid droplets was determined in MCF-10A and MDA-MB-231 cell lines using four normalized LD radii (Figure 9, right). The diameter of the LDs ranged as follows: type 1, 0.33 µm, type 2 (2-fold diameter) 0.67 µm, type 4 (4-fold diameter) 1.3 µm and type 6 (6-fold diameter) 2 µm. During co-culture time, the number of LDs in MCF-10A cells does not increase, but the lipid droplets grow in volume. When MCF-10A cells are not grown in the vicinity of fatty connective tissue, the average LD size distribution is unaltered. In the case of MDA-MB-231 cells, the number of lipid droplets increases in the first three days. Afterwards, the number of lipid droplets remains approximately constant, and the lipid droplets grow in volume. When MDA-MB-231 cells are not grown in the vicinity of the fatty connective tissue, the average lipid droplet distribution is unaltered. Since these first findings include only the relative particle size distribution, more accurate experiments that yield the absolute size and the distributions of the amount of LDs in BC cell lines are planned for future experiments.

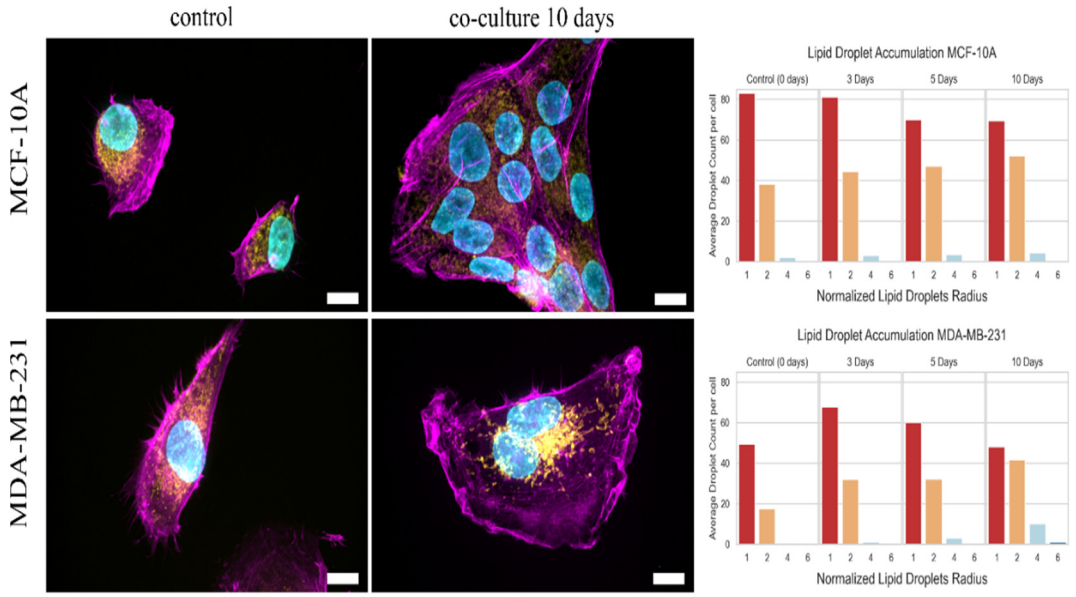

Figure 9. Microscopic images of breast cancer cell lines. (**Left**): MCF-10A (upper images) and MDA-MB 231 (lower images) cells grown without fatty tissue (left images) and after 10 days of co-culture with primary fatty tissue (right images). The scale bar is 10 µm. The amount of lipid droplets (yellow) does not change significantly for the MCF-10A cells. For the MDA-MB-231 cell, on the other hand, the amount and the size of lipid droplets increases after 10 days of co-culture. Yellow: the lipid stain LipidTox Green predominantly stains the endoplasmic reticulum. Blue: cell nuclei stained with SPY-DNA 555. Pink: actin stained with SiR-Actin. (**Right**): lipid droplet accumulation over time in MCF-10A cells (upper image) when exposed to co-cultured fatty tissue. The lipid droplet size is normalized to the smallest lipid droplets of the cell cohort.

4. Conclusions

LD-related genes are associated with overall survival and metastatic stages, and play an essential role in the dynamics of LD in breast cancer patients. Bioinformatics analyses provided key facts for future proteomics and down-regulated functions and pathway analysis by identifying prognostic LD-related genes that may affect metastasis transitions. These findings may help to estimate the role of identified genes in tumorigenesis and metastatic aggressiveness. This was supported by a combination of diverse bioinformatics analyses, cell culture studies, and MS analyses. Although the MS analysis of apolar lipids is not very straightforward, the results indicated major changes in the phospholipids, in particular the chain length and the double-bond content. These changes may be indicative of the conversion of normal cells into tumor cells. Given that the rapid progression of cancer in patients is influenced by multiple factors, the analysis could result in essential indicators of the responsible genes (and accordingly, the selected enzymes) for the rapid progression of metastasis in patients. Future experiments will enable a deeper look into the quantitative lipid distribution between the cell lines, and a proteomic analysis of selected proteins and lipids, aiming to bridge the gap between these two different research fields.

Supplementary Materials: The following supporting information can be downloaded at: https://www.mdpi.com/article/10.3390/lipidology1010005/s1, Supplement S1: PubMed database publications, 143 lipid- and lipid droplet-related genes, their functions, and references list; Supplement S2: Full gene list and their expression comparisons. OS, Expression, F-Value and Metastatic *p*-Value of 143 genes and their comparison; Supplement S3: All overall survival-related genes and their results. Additional 18 genes which show OS and their detailed results; Supplement S4: F-value-related genes and their scores, 14 additional genes, the F-values of which are very high, and their comparison; Supplement S5: Disease-Free Survival genes and their results, nine additional genes show DFS in breast cancer; Supplement S6: Expression of FABP7 in different cancer types and comparison with each other; Supplement S7: Expression of FABP7 in breast cancer subtypes and lineage subtypes.

Author Contributions: S.D. performed the gene bioinformatics analysis, combined biochemistry and biophysics perspectives and conceptualized the manuscript. J.L. performed the gene selection related to lipid metabolism and performed the lipid structure studies. J.S. performed the gene selection analysis and connected lipid wet-lab studies with dry-lab bioinformatics. D.T.H. stained and distinguished the lipid droplets in the cell line cultures and worked on formatting the manuscript. H.K. imaged lipid droplet amounts and their sizes under microscopy. E.B. and A.Z. stained the lipid droplets and evaluated the size and amount of lipid droplets under microscope in breast cancer cell lines. C.F. designed and helped with cell culture. J.A.K. supervised the study. All authors have read and agreed to the published version of the manuscript.

Funding: This study was supported by the German Research Council (DFG Schi 476/19-1, and DFG KA 1116/22-1).

Institutional Review Board Statement: Ethics approval and consent to participate not applicable.

Informed Consent Statement: Informed consent was obtained from all subjects involved in the study.

Data Availability Statement: All data generated or analyzed during this study are included in this article.

Acknowledgments: We are thankful for DFG for supporting our scientific research.

Conflicts of Interest: The authors have no conflicts of interest.

Abbreviations

ACADS: Acyl-CoA Dehydrogenase Short Chain, APOBEC3G: Apolipoprotein B MRNA Editing Enzyme Catalytic Subunit, AQP7: Aquaporin, CAV1: Caveolin, CHKA: Choline Kinase Alpha, CHKB: Choline Kinase Beta, CIDEA: Cell-Death-Inducing DFFA-Like Effector, CPA4, CXCR6, DGAT1, ELOVL1: Fatty Acid Elongase, FABP4: Fatty-Acid-Binding Protein, FITM1: Fat-Storage-Inducing Transmembrane Protein, FKBP5: Prolyl Isomerase, FOXO2: Forkhead Box, HSD: Hydroxysteroid, HSD17B1: Hydroxysteroid 17-Beta Dehydrogenase, LIPE: Lipase E, LPCAT: Lysophosphatidylcholine Acyltransferase, LAMP2: Lysosomal-Associated Membrane Protein, LRGUK: Leucine-Rich Repeats And Guanylate Kinase Domain, LSS: Lanosterol Synthase, MTTP: Microsomal triglyceride transfer protein, OSBPL: Oxysterol-binding protein-like, PIM2: Pim-2 Proto-Oncogene, PLA2G10: Phospholipase A2 Group, PLIN: Perilipin, PNPLA2: Patatin-like phospholipase, PTGS2: Prostaglandin-Endoperoxide Synthase, RBP4: Retinol-Binding Protein, SAA4: Serum Amyloid, SELE: Selectin, SNAP23: Synaptosome-Associated Protein, SQLE: Squalene epoxidase, TMEM229B: Transmembrane Protein.

Summary of background knowledge

Cell Lines: MCF 10A is an epithelial cell line that was isolated in 1984 from the mammary gland of a white, 36-year-old female with fibrocystic breasts. This cell line was deposited by the Michigan Cancer Foundation. **The MDA-MB-231** cell line is an epithelial, human breast cancer cell line, which was established from a pleural effusion of a 51-year Caucasian female with a metastatic mammary adenocarcinoma, and is one of the most commonly used breast cancer cell lines in medical research laboratories. **MDA-MB-436** is a triple-negative breast cancer cell line, which are epithelial in nature.

Statistics: Overall Survival: Survival analysis is a collection of statistical procedures relating to the length of time from either the date of diagnosis or the start of treatment for a disease such as cancer, which patients are diagnosed with, up to death. It is used to estimate the lifespan of a particular population under study. In the beginning, the survival probability is 1.0 (or, 100% of the participants are alive). After that, it gives the probability that a patient, device, or other objects of interest will survive past a certain time [43]. **Cox regression:** This is a method for investigating the effects of a few variables upon the time a specified event takes to happen. It is known as Cox regression for survival analysis if the context outcome is death. The probabilities lower than 0.05 are considered significant and researchers conventionally provide a 95% confidence interval for the hazard ratio [44]. **Hazard Ratio:** This is the hazard rate corresponding to the conditions described by two levels of an explanatory variable. The measures of association tell us that a hazard ratio of 1 means a lack of association, a hazard ratio greater than 1 suggests an increased risk, and a hazard ratio below 1 suggests a smaller risk [45]. **F-Statistics:** this is a statistical test that shows the equality of the variances of the two normal populations and is used to determine whether the variances of two populations

are equal or not, by using a one-tailed or two-tailed hypothesis test [46]. **Disease-Free Survival:** This is a number that shows the chances of staying free of a disease or cancer after a particular treatment. It also refers to the time from treatment until the recurrence of disease (or death) after undergoing curative-intent treatment [47]. **Prognostic Factor:** this is a characteristic of a patient that can be used to estimate the chance of recovery from a disease or the chance of the disease recurring (coming back) [48].

Metastatic Stages in Breast Cancer, According to [32]: **Stage IA**: in this stage, the tumor is characterized by its small size, invasiveness, and absence of spread to the lymph nodes (T1, N0, and M0). **Stage IB**: Cancer has extended to the lymph nodes, with the size of the cancerous lymph node falling between 0.2 mm and less than 2 mm. There is either no presence of a tumor in the breast, or, if there is, it measures 20 mm or smaller (T0 or T1, N1mi, and M0).**Stage IIA**: This stage includes various conditions, such as the absence of a tumor in the breast but the presence of cancer in one-to-three axillary lymph nodes, with no distant spread (T0, N1, and M0). Additionally, a tumor measuring 20 mm or smaller that has spread to one-to-three axillary lymph nodes (T1, N1, and M0), or a tumor larger than 20 mm but not exceeding 50 mm without spread to axillary lymph nodes (T2, N0, and M0). **Stage IIB**: This stage encompasses scenarios where the tumor is larger than 20 mm but not exceeding 50 mm, with spread to one-to-three axillary lymph nodes (T2, N1, and M0). Alternatively, the tumor is larger than 50 mm without spreading to axillary lymph nodes (T3, N0, M0). **Stage IIIA**: Tumors of any size in this stage have spread to four-to-nine axillary lymph nodes or internal mammary lymph nodes, but not to other parts of the body (T0, T1, T2, or T3; N2; and M0). Stage IIIA may also involve a tumor larger than 50 mm that has spread to one-to-three axillary lymph nodes (T3, N1, and M0). **Stage IIIB**: The tumor has spread to the chest wall, caused swelling or ulceration of the breast, or has been diagnosed as inflammatory breast cancer. It may or may not have spread to up to nine axillary or internal mammary lymph nodes, but has not extended to other body parts (T4; N0, N1, or N2; and M0). **Stage IIIC**: In this stage, tumors of any size have spread to 10 or more axillary lymph nodes, internal mammary lymph nodes, and/or lymph nodes under the collarbone. Importantly, there is no spread to other parts of the body (any T, N3, and M0). **Stage IV** (metastatic): The tumor, regardless of size, has metastasized to organs like the bones, lungs, brain, liver, distant lymph nodes, or chest wall (any T, any N, and M1). De novo metastatic breast cancer, discovered at the initial diagnosis, accounts for approximately 6% of cases, while metastatic breast cancer is more commonly identified after prior diagnosis and treatment of early-stage breast cancer.

References

1. Bray, F.; Ferlay, J.; Soerjomataram, I.; Siegel, R.L.; Torre, L.A.; Jemal, A. Global cancer statistics 2018: GLOBOCAN estimates of incidence and mortality worldwide for 36 cancers in 185 countries. *CA Cancer J. Clin.* **2018**, *68*, 394–424. [CrossRef]
2. World Health Organization: Breast Cancer. 2021. Available online: www.who.int/news-room/fact-sheets/detail/breast-cancer (accessed on 21 April 2023).
3. Rositch, A.F.; Unger-Saldaña, K.; DeBoer, R.J.; Ng'ang'a, A.; Weiner, B.J. The role of dissemination and implementation science in global breast cancer control programs: Frameworks, methods, and examples. *Cancer* **2020**, *126* (Suppl. S10), 2394–2404. [CrossRef]
4. Ginsburg, O.; Yip, C.-H.; Brooks, A.; Cabanes, A.; Caleffi, M.; Dunstan Yataco, J.A.; Gyawali, B.; McCormack, V.; de Anderson, M.M.; Mehrotra, R.; et al. Breast cancer early detection: A phased approach to implementation. *Cancer* **2020**, *126* (Suppl. S10), 2379–2393. [CrossRef]
5. Provenzano, E.; Ulaner, G.A.; Chin, S.-F. Molecular Classification of Breast Cancer. *PET Clin.* **2018**, *13*, 325–338. [CrossRef]
6. Cavallaro, S.; Paratore, S.; de Snoo, F.; Salomone, E.; Villari, L.; Buscarino, C.; Ferraù, F.; Banna, G.; Furci, M.; Strazzanti, A.; et al. Genomic analysis: Toward a new approach in breast cancer management. *Crit. Rev. Oncol. Hematol.* **2012**, *81*, 207–223. [CrossRef]
7. Kim, M.; Park, J.; Bouhaddou, M.; Kim, K.; Rojc, A.; Modak, M.; Soucheray, M.; McGregor, M.J.; O'leary, P.; Wolf, D.; et al. A protein interaction landscape of breast cancer. *Science* **2021**, *374*, eabf3066. [CrossRef]
8. Núñez, C. Blood-based protein biomarkers in breast cancer. *Clin. Chim. Acta.* **2019**, *490*, 113–127. [CrossRef]
9. Callesen, A.K.; Madsen, J.S.; Vach, W.; Kruse, T.A.; Mogensen, O.; Jensen, O.N. Serum protein profiling by solid phase extraction and mass spectrometry: A future diagnostics tool? *Proteomics* **2009**, *9*, 1428–1441. [CrossRef]
10. Veyssière, H.; Bidet, Y.; Penault-Llorca, F.; Radosevic-Robin, N.; Durando, X. Circulating proteins as predictive and prognostic biomarkers in breast cancer. *Clin. Proteom.* **2022**, *19*, 25. [CrossRef] [PubMed]
11. Rajkumar, T.; Amritha, S.; Sridevi, V.; Gopal, G.; Sabitha, K.; Shirley, S.; Swaminathan, R. Identification and validation of plasma biomarkers for diagnosis of breast cancer in South Asian women. *Sci. Rep.* **2022**, *12*, 100. [CrossRef] [PubMed]
12. Uehiro, N.; Sato, F.; Pu, F.; Tanaka, S.; Kawashima, M.; Kawaguchi, K.; Sugimoto, M.; Saji, S.; Toi, M. Circulating cell-free DNA-based epigenetic assay can detect early breast cancer. *Breast Cancer Res.* **2016**, *18*, 129. [CrossRef] [PubMed]
13. Han, X.; Gross, R.W. Global analyses of cellular lipidomes directly from crude extracts of biological samples by ESI mass spectrometry: A bridge to lipidomics. *J. Lipid Res.* **2003**, *44*, 1071–1079. [CrossRef] [PubMed]

14. Schröter, J.; Popkova, Y.; Süß, R.; Schiller, J. Combined use of MALDI-TOF mass spectrometry and 31P NMR spectroscopy for analysis of phospholipids. *Methods Mol. Biol.* **2017**, *1609*, 107–122. [CrossRef] [PubMed]
15. Guo, R.; Chen, Y.; Borgard, H.; Jijiwa, M.; Nasu, M.; He, M.; Deng, Y. The function and mechanism of lipid molecules and their roles in the diagnosis and prognosis of breast cancer. *Molecules* **2020**, *25*, 4864. [CrossRef]
16. Silva, C.L.; Perestrelo, R.; Sousa-Ferreira, I.; Capelinha, F.; Câmara, J.S.; Petković, M. Lipid biosignature of breast cancer tissues by matrix-assisted laser desorption/ionization time-of-flight mass spectrometry. *Breast Cancer Res. Treat.* **2020**, *182*, 9–19. [CrossRef] [PubMed]
17. Lee, Y.J.; Shin, K.J.; Jang, H.-J.; Noh, D.-Y.; Ryu, S.H.; Suh, P.-G. Phospholipase signaling in breast cancer. *Adv. Exp. Med. Biol.* **2021**, *1187*, 23–52. [CrossRef] [PubMed]
18. Tőkés, A.M.; Vári-Kakas, S.; Kulka, J.; Törőcsik, B. Tumor glucose and fatty acid metabolism in the context of anthracycline and taxane-based (neo)adjuvant chemotherapy in breast carcinomas. *Front. Oncol.* **2022**, *12*, 850401. [CrossRef] [PubMed]
19. Menendez, J.A.; Lupu, R. Fatty acid synthase: A druggable driver of breast cancer brain metastasis. *Expert. Opin. Ther. Targets.* **2022**, *26*, 427–444. [CrossRef] [PubMed]
20. Li, Y.-L.; Tian, H.; Jiang, J.; Zhang, Y.; Qi, X.-W. Multifaceted regulation and functions of fatty acid desaturase 2 in human cancers. *Am. J. Cancer Res.* **2020**, *10*, 4098–4111.
21. Cruz, A.L.S.; Barreto, E.d.A.; Fazolini, N.P.B.; Viola, J.P.B.; Bozza, P.T. Lipid droplets: Platforms with multiple functions in cancer hallmarks. *Cell Death Dis.* **2020**, *11*, 105. [CrossRef]
22. Liu, X.; Zhang, P.; Xu, J.; Lv, G.; Li, Y. Lipid metabolism in tumor microenvironment: Novel therapeutic targets. *Cancer Cell Int.* **2022**, *22*, 224. [CrossRef] [PubMed]
23. Rustan, A.C.; Drevon, C.A. Fatty Acids: Structures and Properties. In *Encyclopedia of Life Sciences*; Wiley: Weinheim, Germany, 2005. [CrossRef]
24. Folch, J.; Lees, M.; Sloane Stanley, G.H. A simple method for the isolation and purification of total lipides from animal tissues. *J. Biol. Chem.* **1957**, *226*, 497–509. [CrossRef]
25. Tang, Z.; Li, C.; Kang, B.; Gao, G.; Li, C.; Zhang, Z. GEPIA: A web server for cancer and normal gene expression profiling and interactive analyses. *Nucleic Acids Res.* **2017**, *45*, W98–W102. [CrossRef] [PubMed]
26. Shen, Y.; Schmidt, B.U.S.; Kubitschke, H.; Morawetz, E.W.; Wolf, B.; Käs, J.A.; Losert, W. Detecting heterogeneity in and between breast cancer cell lines. *Cancer Converg.* **2020**, *4*, 1. [CrossRef] [PubMed]
27. Fuchs, B.; Schiller, J.; Süss, R.; Schürenberg, M.; Suckau, D. A direct and simple method of coupling matrix-assisted laser desorption and ionization time-of-flight mass spectrometry (MALDI-TOF MS) to thin-layer chromatography (TLC) for the analysis of phospholipids from egg yolk. *Anal. Bioanal. Chem.* **2007**, *389*, 827–834. [CrossRef] [PubMed]
28. Bui, Q.; Sherma, J.; Hines, J.K. Using high performance thin layer chromatography-densitometry to study the influence of the prion RNQ+ and its determinant prion protein Rnq1 on yeast lipid profiles. *Separations* **2018**, *5*, 6. [CrossRef] [PubMed]
29. Klöting, N.; Fasshauer, M.; Dietrich, A.; Kovacs, P.; Schön, M.R.; Kern, M.; Stumvoll, M.; Blüher, M. Insulin-sensitive obesity. *Am. J. Physiol. Endocrinol. Metab.* **2010**, *299*, E506-15. [CrossRef]
30. Schmitz, J.; Evers, N.; Awazawa, M.; Nicholls, H.T.; Brönneke, H.S.; Dietrich, A.; Mauer, J.; Blüher, M.; Brüning, J. Obesogenic memory can confer long-term increases in adipose tissue but not liver inflammation and insulin resistance after weight loss. *Mol. Metab.* **2016**, *5*, 328–339. [CrossRef] [PubMed]
31. Eggert, D.; Rösch, K.; Reimer, R.; Herker, E. Visualization and analysis of hepatitis C virus structural proteins at lipid droplets by super-resolution microscopy. *PLoS ONE* **2014**, *9*, e102511. [CrossRef]
32. Available online: https://www.cancercenter.com/cancer-types/breast-cancer/stage (accessed on 15 January 2024).
33. Amin, M.B.; Greene, F.L.; Edge, S.B. (Eds.) *AJCC Cancer Staging Manual*; AJCC American Joint Committee on Cancer: Chicago, IL, USA; Springer: Berlin/Heidelberg, Germany, 2017.
34. Chang, X.; Xing, P. Identification of a novel lipid metabolism-related gene signature within the tumour immune microenvironment for breast cancer. *Lipids Health Dis.* **2022**, *21*, 43. [CrossRef]
35. White, T.; Bursten, S.; Federighi, D.; Lewis, R.A.; Nudelman, E. High-resolution separation and quantification of neutral lipid and phospholipid species in mammalian cells and sera by multi-one-dimensional thin-layer chromatography. *Anal. Biochem.* **1998**, *258*, 109–117. [CrossRef] [PubMed]
36. Wang, H.-Y.J.; Huang, C.-Y.; Wei, K.-C.; Hung, K.-C. A mass spectrometry imaging and lipidomic investigation reveals aberrant lipid metabolism in the orthotopic mouse glioma. *J. Lipid Res.* **2022**, *63*, 100304. [CrossRef] [PubMed]
37. Giudetti, A.M.; De Domenico, S.; Ragusa, A.; Lunetti, P.; Gaballo, A.; Franck, J.; Simeone, P.; Nicolardi, G.; De Nuccio, F.; Santino, A.; et al. A specific lipid metabolic profile is associated with the epithelial mesenchymal transition program. *Biochim. Biophys. Acta Mol. Cell Biol. Lipids.* **2019**, *1864*, 344–357. [CrossRef] [PubMed]
38. Ohno, Y.; Suto, S.; Yamanaka, M.; Mizutani, Y.; Mitsutake, S.; Igarashi, Y.; Sassa, T.; Kihara, A. ELOVL1 production of C24 acyl-CoAs is linked to C24 sphingolipid synthesis. *Proc. Natl. Acad. Sci. USA* **2010**, *107*, 18439–18444. [CrossRef]
39. Adler, D.H.; Cogan, J.D.; Phillips, J.A.; Schnetz-Boutaud, N.; Milne, G.L.; Iverson, T.; Stein, J.A.; Brenner, D.A.; Morrow, J.D.; Boutaud, O.; et al. Inherited human cPLA(2alpha) deficiency is associated with impaired eicosanoid biosynthesis, small intestinal ulceration, and platelet dysfunction. *J. Clin. Investig.* **2008**, *118*, 2121–2131. [CrossRef]
40. Balendiran, G.K.; Schnutgen, F.; Scapin, G.; Borchers, T.; Xhong, N.; Lim, K.; Godbout, R.; Spener, F.; Sacchettini, J.C. Crystal structure and thermodynamic analysis of human brain fatty acid-binding protein. *J. Biol. Chem.* **2000**, *275*, 27045–27054. [CrossRef]

41. Tschodu, D.; Ulm, B.; Bendrat, K.; Lippoldt, J.; Gottheil, P.; Käs, J.A.; Niendorf, A. Comparative analysis of molecular signatures reveals a hybrid approach in breast cancer: Combining the nottingham prognostic index with gene expressions into a hybrid signature. *PLoS ONE* **2022**, *17*, e0261035. [CrossRef]
42. Vidavsky, N.; Kunitake, J.A.M.R.; Diaz-Rubio, M.E.; Chiou, A.E.; Loh, H.-C.; Zhang, S.; Masic, A.; Fischbach, C.; Estroff, L.A. Mapping and profiling lipid distribution in a 3D model of breast cancer progression. *ACS Cent. Sci.* **2019**, *5*, 768–780. [CrossRef]
43. Hajihosseini, M.; Faradmal, J.; Sadighi-Pashaki, A. Survival analysis of breast cancer patients after surgery with an intermediate event: Application of illness-death model. *Iran. J. Public Health* **2015**, *44*, 1677–1684.
44. Abadi, A.; Yavari, P.; Dehghani-Arani, M.; Alavi-Majd, H.; Ghasemi, E.; Amanpour, F.; Bajdik, C. Cox models survival analysis based on breast cancer treatments. *Iran. J. Cancer Prev.* **2014**, *7*, 124–129.
45. Hilsenbeck, S.G.; Ravdin, P.M.; Moor CA de Chamness, G.C.; Osborne, C.K.; Clark, G.M. Time-dependence of hazard ratios for prognostic factors in primary breast cancer. *Breast Cancer Res. Treat.* **1998**, *52*, 227–237. [CrossRef] [PubMed]
46. Markowski, C.A.; Markowski, E.P. Conditions for the effectiveness of a preliminary test of variance. *Am. Statistician.* **1990**, *44*, 322. [CrossRef]
47. Paik, H.-J.; Lee, S.K.; Ryu, J.M.; Park, S.; Kim, I.; Bae, S.Y.; Yu, J.; Lee, J.E.; Kim, S.W.; Nam, S.J. Conditional disease-free survival among patients with breast cancer. *Medicine* **2017**, *96*, e5746. [CrossRef] [PubMed]
48. Phung, M.T.; Tin Tin, S.; Elwood, J.M. Prognostic models for breast cancer: A systematic review. *BMC Cancer* **2019**, *19*, 230. [CrossRef] [PubMed]